WAPRIME

https://welchacademy.com/index.php/prime

e-ISSN: 3062-2743

Experimental analysis of ultrasonic testing applications using straight beam and angle beam probes

Cenap Güven [*1], **Cengiz Doğan** [2]

[1] *Harran University, Vocational School of Technical Sciences, Department of Electronics and Automation, Türkiye, cenap_guven@harran.edu.tr*
[2] *Harran University, Engineering Faculty, Department of Mechanical Engineering, Türkiye, cdogan@harran.edu.tr*

Cite this study: Güven, C., & Doğan, C. (2025). Experimental analysis of ultrasonic testing applications using straight beam and angle beam probes. WAPRIME, 2(2), 55-69.

https://doi.org/10.5281/zenodo.18300070

Keywords

Ultrasonic Testing Device
Probe
Specimen
Transducer

Research Article

Received: 30 November 2025
Revised: 27 December 2025
Accepted: 28 December 2025
Published: 31 December 2025

Abstract

This study presents a thorough experimental comparison of the performance between standard ultrasonic probes and angled probes in ultrasonic testing applications. Additionally, it investigates the impressive potential of standard probes to generate wave propagation similar to that of angled probes when optimal geometric and acoustic configurations are utilized. Through carefully designed experiments, we analyzed the echo signals obtained from both types of probes, focusing on key factors such as signal amplitude, wave entry angle, defect detection capabilities, and measurement repeatability. Notably, during contact tests, we observed fluctuations in signal stability and challenges posed by the proximity of defects to the surface. These observations were closely related to the surface condition and the interaction between the probe and the sample. In contrast, tests conducted in water resulted in significantly more stable and repeatable outcomes. Our investigation demonstrated that when using a standard probe for angled scans in water, both longitudinal and transverse waves were effectively generated. To achieve optimal inspection with transverse waves, it was crucial to adjust the probe within a specific angle range. The findings of this study provide strong evidence that, under certain conditions, standard probes can serve as a viable and cost-effective alternative to angled probes. However, it is important to acknowledge that traditional angled probes continue to excel in applications requiring high sensitivity. This research advocates for a novel approach that harnesses standard probes in angled testing for non-destructive testing applications, thereby establishing a scientific foundation for alternative, economical solutions that could advance practices in the field.

1. Introduction

Ultrasonic Testing (UT) remains a cornerstone of non-destructive evaluation (NDE). It operates on the fundamental principle of propagating high-frequency mechanical waves through a medium to scrutinize reflections from internal discontinuities, grain boundaries, or geometric interfaces [1-3]. The versatility of UT facilitates its widespread adoption across a diverse industrial spectrum, particularly for detecting deep-seated defects, gauging thickness, and ensuring the structural integrity of weldments [4-8]. When compared to competing

NDE modalities, UT is distinguished by its exceptional penetration depth, high spatial resolution, and the capacity for instantaneous diagnostic feedback [9-11].

The efficacy of ultrasonic inspection is largely dictated by probe configuration, typically bifurcated into normal (straight-beam) and angle-beam transducers [1, 12]. Normal probes primarily induce longitudinal waves perpendicular to the entry surface, making them the gold standard for thickness profiling and the detection of laminar defects. In contrast, angle-beam probes—leveraging specialized wedges to generate refracted shear waves—are indispensable for identifying misaligned flaws and root defects in complex welded geometries [13, 14]. Despite their critical role, the industrial deployment of angle-beam probes is often hampered by elevated costs, the necessity for extensive inventories, and restricted maneuverability in confined spaces. Such constraints have catalyzed a shift toward investigating alternative acoustic configurations. Consequently, evaluating whether normal probes can emulate the performance of angle-beam transducers through strategic geometric and acoustic optimizations has emerged as a pivotal research frontier.

Optimizing wave transmission requires a stable acoustic coupling medium between the transducer and the specimen. This requirement divides UT methodologies into two primary paradigms: contact and immersion testing. In contact testing, a couplant—typically gel or oil—facilitates direct interface [8, 15]. While prioritized in field operations for its logistical simplicity, this approach is susceptible to signal attenuation and inconsistent coupling due to surface topography. Conversely, immersion UT mitigates these limitations by submerging the components in a water bath, where water serves as a highly stable transmission medium [1, 3]. This setup eliminates air-borne losses and grants the practitioner unprecedented precision over the incident wave angle [16]. Consequently, immersion UT is the preferred modality for automated high-fidelity scanning and rigorous experimental investigations.

This study presents an experimental interrogation into the comparative performance of normal and angle-beam probes under both contact and immersion regimes. We specifically examine the potential of normal probes to generate angled wave profiles, assessing their efficacy through signal amplitude analysis, echo characteristics, and flaw-detection sensitivity. By benchmarking these findings against traditional angle-beam benchmarks, this research aims to validate the feasibility of normal probes as a versatile alternative. Furthermore, it elucidates how varying test environments influence measurement accuracy, providing critical data for future NDE protocols.

2. Materials and Methods

In this study, a Starmans DIO 1000 brand ultrasonic device was used. This device can be used with many types of probes and also has the capabilities of drawing DAC curves, performing A, B, and C scans, and connecting to a computer. It can also determine the location and size of discontinuities that may occur in the internal structure of the material, such as gas voids, cracks, slag inclusions, corrosion, erosion, and laminations. Probes with a frequency of 4 MHz were used, including standard probes and probes with angles of 45°, 60°, and 70°. The detailed configuration of the Starmans DIO 1000 unit, along with its specialized probe assembly, is compellingly illustrated in Figure 1.

Figure 1. The Starmans DIO 1000 manual ultrasonic flaw detector and its associated probe assembly.

To ensure high-fidelity data acquisition and eliminate the inconsistencies associated with manual coupling, the ultrasonic instrumentation was integrated into a specialized immersion testing configuration, as depicted in Figure 2 [17].

Figure 2. The ultrasonic flaw detector and the integrated immersion testing assembly [17].

2.1. Experimental Specimen and Setup

The investigation was conducted on a steel test specimen with dimensions of 256×72×57 mm. To simulate internal discontinuities, the specimen was meticulously prepared with artificial side-drilled holes (SDH) of varying diameters—4.5, 5.5, 6.5, and 8.5 mm—positioned strategically at depths of 15, 30, 45, and 60 mm from the superior surface, as illustrated in Figure 3. To ensure optimal acoustic coupling and minimize interface scattering, the specimen surface was first milled and subsequently precision-ground to a surface roughness of R_a=0.8 μm.

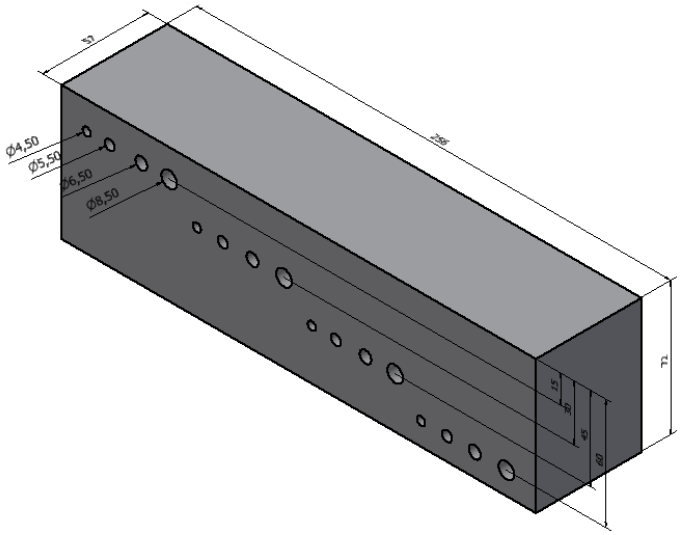

Figure 3. Schematic representation and dimensions of the test specimen featuring artificial side-drilled holes at varying depths and diameters.

Before the immersion testing procedures, the ultrasonic flaw detector was calibrated using standard reference blocks to ensure quantitative accuracy. Following calibration, the specimen was positioned within the previously described immersion tank. To optimize the detection of internal flaws, the ultrasonic gate and time-base settings were adjusted to shift the initial interface echoes (from the water-specimen boundary) out of the primary viewing range. This configuration isolated the signals originating exclusively from the interior of the steel volume, thereby enhancing the signal-to-noise ratio of internal reflections. The strategic positioning of the transducer for defect detection is depicted in Figure 4.

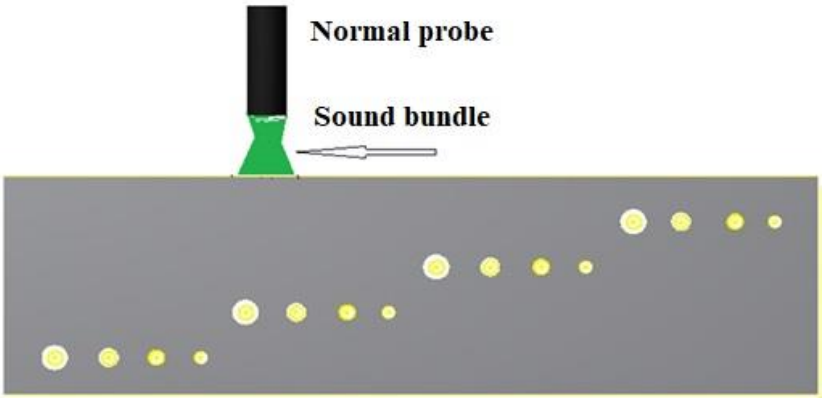

Figure 4. Transducer orientation and scanning trajectory for defect localization within the specimen.

2.2. Secondary Experimental Specimen and Inspection Procedure

A secondary test specimen, measuring 115 x 59 x 38 mm, was fabricated to further evaluate the detection sensitivity across varying depths. As illustrated in Figure 5, the specimen was prepared with side-drilled holes (SDH) of two distinct diameters positioned parallel to the scanning surface. Specifically, 4 mm diameter holes were precision-machined at depths of 11, 29.5, and 48 mm, while 6.5 mm diameter holes were strategically placed at 11 and 48 mm.

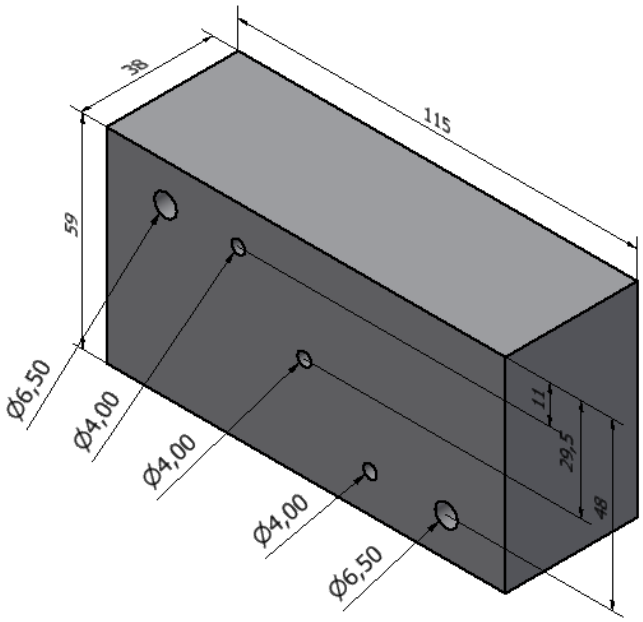

Figure 5. Schematic and dimensional specifications of the secondary 115 x 59 x 38 mm test specimen.

To maintain acoustic consistency with the previous specimen and minimize signal noise, the entry surface was precision-ground to a surface roughness of Ra = 0.8 µm. The ultrasonic inspection of this specimen was performed using a straight-beam (normal) probe configuration, the scanning methodology of which is depicted in Figure 6.

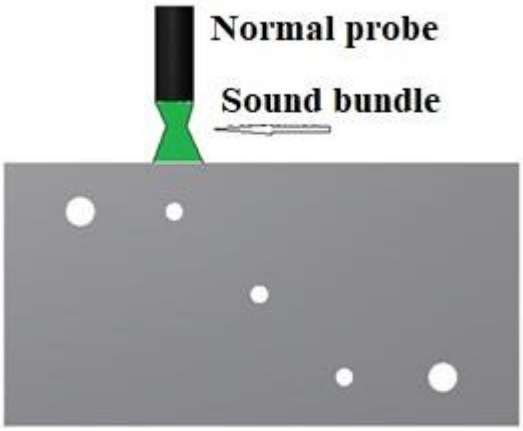

Figure 6. Experimental setup and scanning procedure utilizing a normal (straight-beam) probe on the secondary specimen [17].

2.3. Third Experimental Specimen

The third experimental specimen, with dimensions of 115 x 59 x 38 mm, was fabricated to incorporate internal discontinuities for further sensitivity analysis. As delineated in Figure 7, this specimen features side-drilled holes with a diameter of 4.50 mm, precisely positioned parallel to the entry surface at depths of 12, 30, and 48 mm. The strategic placement of these artificial defects allows for the systematic evaluation of signal response consistency across increasing material thicknesses.

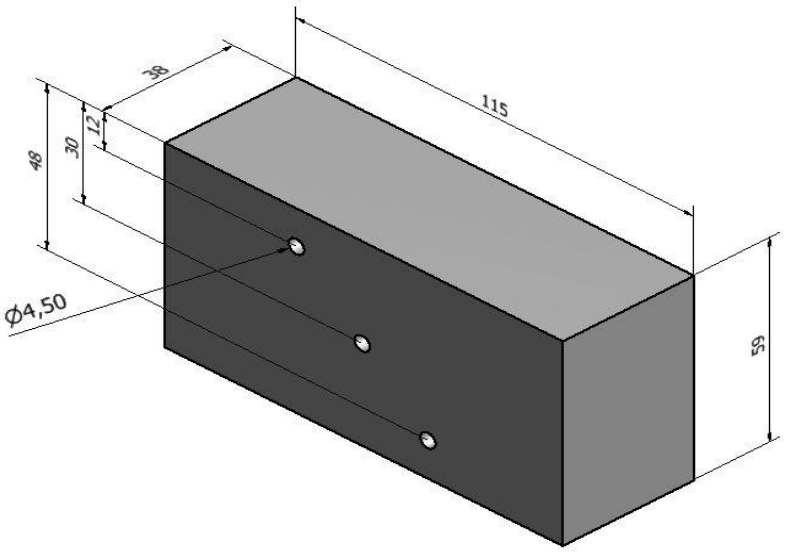

Figure 7. Schematic representation and geometric specifications of the third 115 x 59 x 38 mm test specimen.

2.4. Comparative Flaw Detection via 45° Immersion and Contact Methodologies

To evaluate the efficacy of the proposed method, three side-drilled holes (SDH) with a diameter of 4.5 mm were strategically positioned at depths of 12, 30, and 48 mm within the steel block. The specimen surface was precision-ground to a roughness of Ra=0.7 µm to ensure optimal acoustic transmission. The investigation utilized two distinct ultrasonic testing modalities for comparative analysis. In the first configuration, an immersion testing setup was employed where a normal (straight-beam) probe was oriented as shown in Figure 8a. In accordance with Snell's Law, an incident wave was propagated through the water at an angle of 19◦, calculated to produce a refracted shear wave angle of exactly 45◦ within the steel volume. Conversely, the second methodology involved a conventional contact-based scan utilizing a standard 45-degree◦ angle-beam probe, as illustrated in Figure 8b. This dual-approach setup facilitates a direct performance benchmark between immersion-based angle generation and traditional contact inspection.

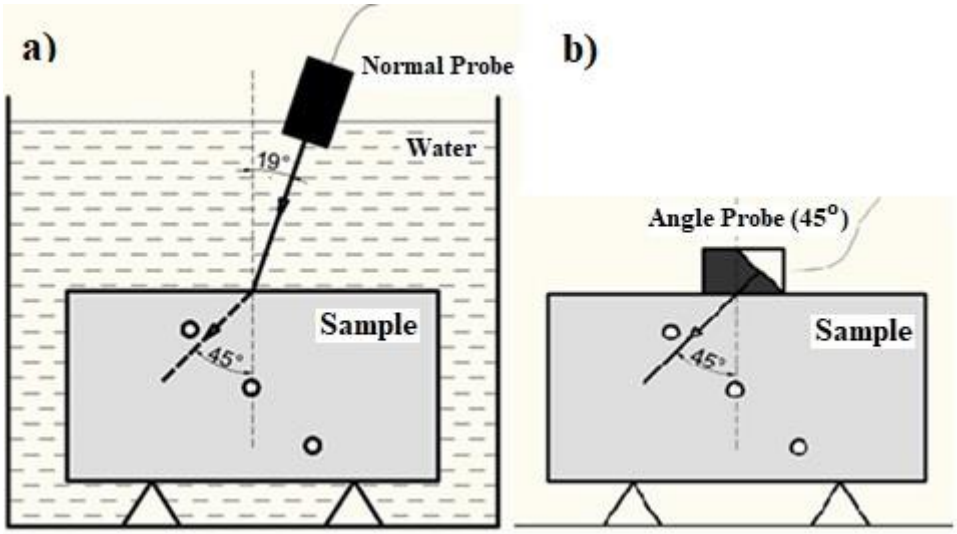

Figure 8. Comparative ultrasonic inspection of the test specimen at a 45° refractive angle: **(a)** Immersion testing configuration utilizing a normal probe with a 19° incident angle; **(b)** Conventional contact testing utilizing a 45° angle-beam probe.

2.5. Comparative Flaw Detection via 60° Refraction: Immersion vs. Contact Methods

The artificial discontinuities within the third specimen were further evaluated using a 60° inspection angle, implemented through two comparative ultrasonic testing modalities. In the first approach, an immersion testing

configuration was utilized as illustrated in Figure 9a. Following the principles of Snell's Law, the normal probe was strategically oriented to propagate an incident wave into the water at an angle of 23°. This incident wave undergoes refraction at the water-steel interface, resulting in a 60° refracted shear wave within the specimen volume. For the second approach, a conventional contact-based scan was performed on the same specimen using a standard 60° angle-beam probe, as shown in Figure 9b. This comparative setup aims to benchmark the signal fidelity and detection sensitivity of the immersion-generated 60° wave against the industry-standard contact method.

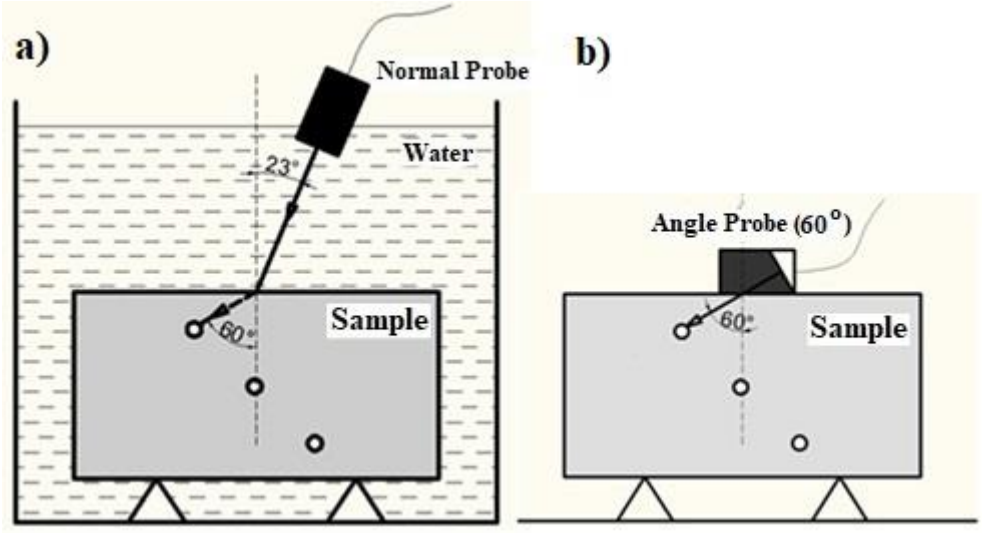

Figure 9. Comparative ultrasonic inspection of the test specimen at a 60° refractive angle: **(a)** Immersion testing configuration utilizing a normal probe with a 23° incident angle; **(b)** Conventional contact testing utilizing a 60° angle-beam probe.

2.6. Comparative Flaw Detection via 70° Refraction: Immersion vs. Contact Methods

The final stage of the comparative analysis involved the interrogation of the third specimen at a 70° refraction angle. Similar to the previous experimental procedures, two distinct ultrasonic testing modalities were implemented. In the immersion testing regime (Figure 10a), the normal (straight-beam) transducer was precisely oriented to propagate an incident wave into the water at an angle of 25°. Governed by Snell's Law, this incident wave undergoes refraction and mode conversion at the water-steel interface, generating a 70° refracted shear wave within the steel specimen. For the second modality, a conventional contact-based scan was executed using a standard 70° angle-beam probe, as illustrated in Figure 10b. This configuration serves to evaluate the detection sensitivity and signal-to-noise ratio of the immersion-based approach at a high refractive angle, which is particularly sensitive to interface conditions.

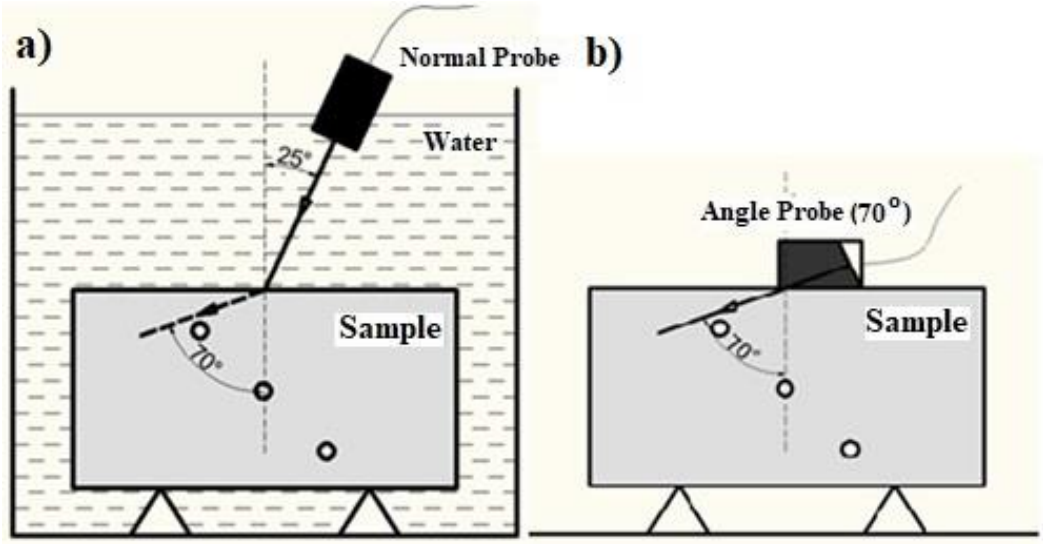

Figure 10. Comparative ultrasonic inspection of the test specimen at a 70° refractive angle: **(a)** Immersion testing configuration utilizing a normal probe with a 25° incident angle; **(b)** Conventional contact testing utilizing a 70° angle-beam probe.

2.6. Fourth Experimental Specimens

The fourth set of experimental specimens comprised three steel blocks, each featuring cross-sectional dimensions of 42 x 36 mm. These blocks were fabricated with varying heights of 30, 49, and 71 mm to facilitate a multi-layered analysis of wave propagation. To ensure high-fidelity acoustic coupling and minimize signal attenuation during the ultrasonic inspection, the contact surfaces of all blocks were precision-ground, as illustrated in Figure 11.

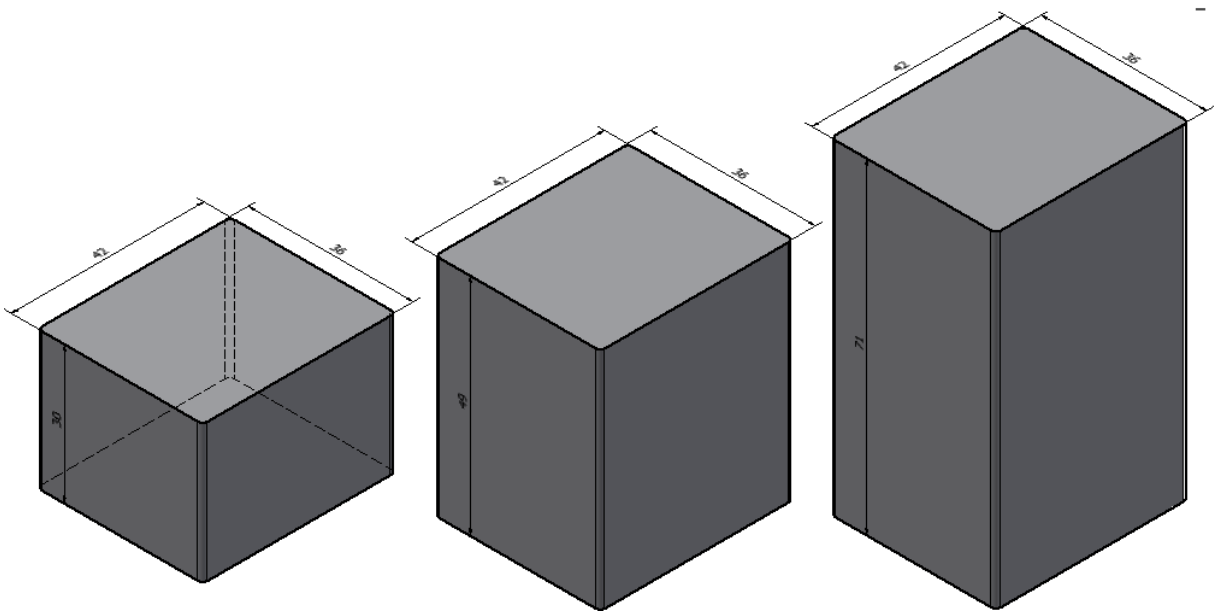

Figure 11. The fourth set of experimental steel specimens with heights of 30, 49, and 71 mm.

2.7. Contact-Based Ultrasonic Inspection of the Fourth Specimen Set

In the initial phase of the experimental evaluation, ultrasonic echo signals were acquired from the fourth specimen set using the conventional contact testing method, as depicted in Figure 12. The inspection was performed on rectangular steel blocks with heights of 30, 49, and 71 mm, each having cross-sectional dimensions of 42 x 36 mm. This procedure aimed to establish baseline longitudinal wave reflections using a normal straight-beam probe, thereby facilitating a comparative analysis of signal response characteristics across varying material thicknesses.

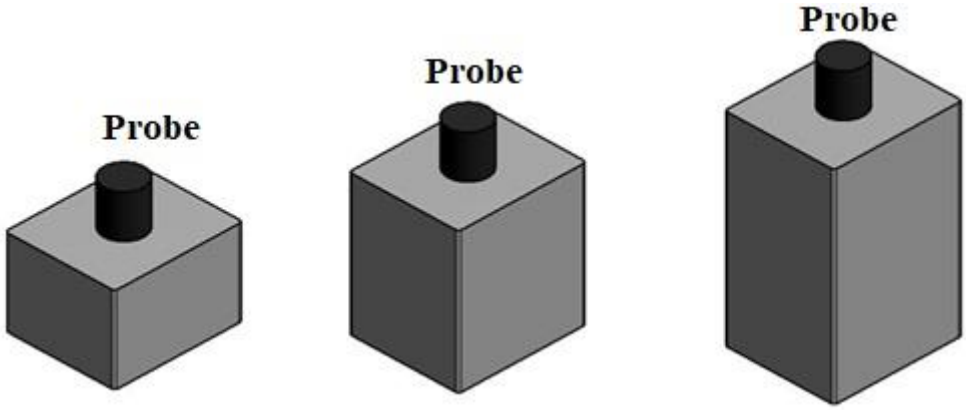

Figure 12. Experimental configuration for the contact-based ultrasonic inspection of the fourth specimen set utilizing a normal straight-beam probe.

2.8. Immersion-Based Ultrasonic Inspection of the Fourth Specimen Set

The subsequent phase of the experimental protocol involved the immersion-based inspection of the identical steel specimens, as illustrated in Figure 13. Utilizing the same normal (straight-beam) transducer, the scanning procedure was performed within the water tank while maintaining a constant water path (stand-off distance) of 18 mm between the probe face and the specimen's entry surface. This immersion configuration was strategically established to provide a stable and uniform acoustic coupling environment, ensuring high-fidelity wave propagation and allowing for the precise evaluation of echo characteristics under controlled immersion conditions.

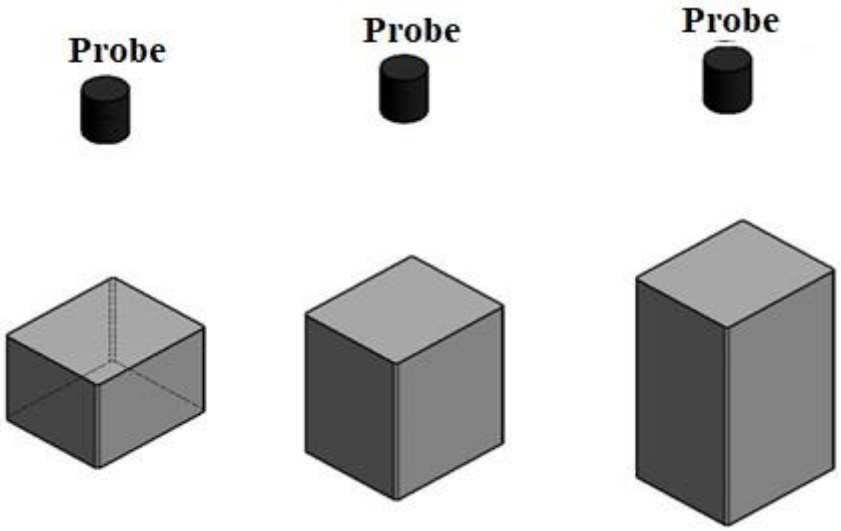

Figure 13. Experimental configuration for the contact-based ultrasonic inspection of the fourth specimen set utilizing a normal straight-beam probe.

3. Results and Discussion

3.1. Analysis of Flaw Detection in Specimen 1 via Normal Incidence Immersion Testing

The correlation between signal amplitude and flaw parameters in the first specimen was evaluated using referance+ incidence immersion testing, with the resulting data summarized in Figure 14. To establish a baseline for the scanning procedure, the instrumentation was normalized by setting the echo from the 8.5 mm diameter hole (at a depth of 15 mm) to a 100% full-screen height (FSH) reference. A systematic analysis of the graphical data reveals a clear attenuation of signal amplitude as a function of both increasing depth and decreasing defect diameter. Specifically, for the 8.5 mm holes, the amplitude dropped from 100% at a depth of 15 mm to 46% at 60

mm. For the 6.5 mm diameter holes, the signal intensity decreased from 79% to 28% over the same depth interval. A similar trend was observed for the 5.5 mm and 4.5 mm diameter holes, where amplitudes declined from 74% to 20% and from 65% to 16%, respectively. These empirical results confirm that signal amplitude is directly proportional to the cross-sectional area of the discontinuity and inversely proportional to its distance from the transducer, consistent with the principles of ultrasonic beam divergence and material attenuation.

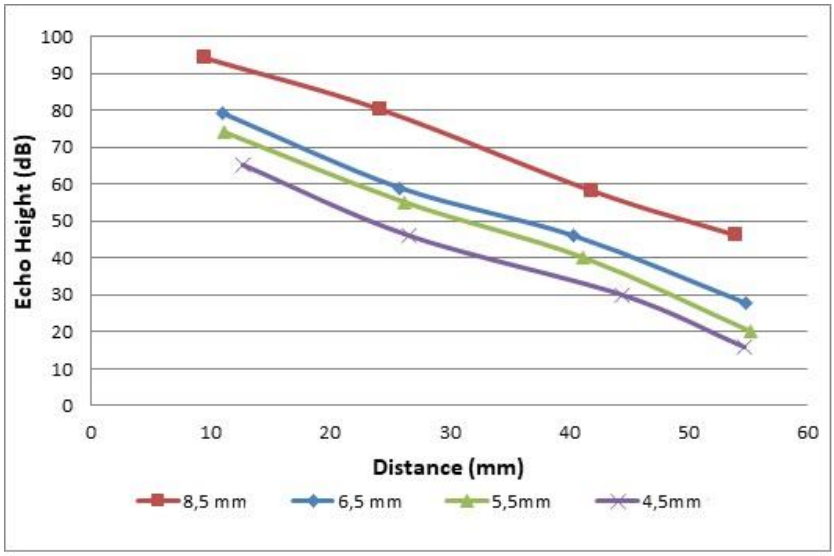

Figure 14. Experimental findings illustrating the relationship between signal amplitude, flaw diameter, and depth for the first specimen during immersion testing.

3.2. Evaluation of Flaw Detection in Specimen 2 via Normal Incidence Immersion Testing

The second specimen was interrogated using a normal probe under immersion conditions, mirroring the experimental configuration and positional parameters employed for the first specimen. To standardize the amplitude measurements, the echo signal originating from the 6.5 mm diameter hole at a depth of 11 mm was designated as the 100% Full-Screen Height (FSH) reference. The empirical findings, as illustrated in Figure 15, demonstrate a systematic attenuation of the ultrasonic signal relative to depth and diameter. Specifically, for the 6.5 mm diameter hole, the signal amplitude decreased from its reference peak to 48% at a depth of 48 mm. In comparison, the 4 mm diameter hole yielded a signal height of 85% at an 11 mm depth, which subsequently attenuated to 40% at 48 mm. These results further corroborate the predictable decay of acoustic energy and highlight the sensitivity of the immersion methodology in resolving flaws of varying dimensions across different material thicknesses.

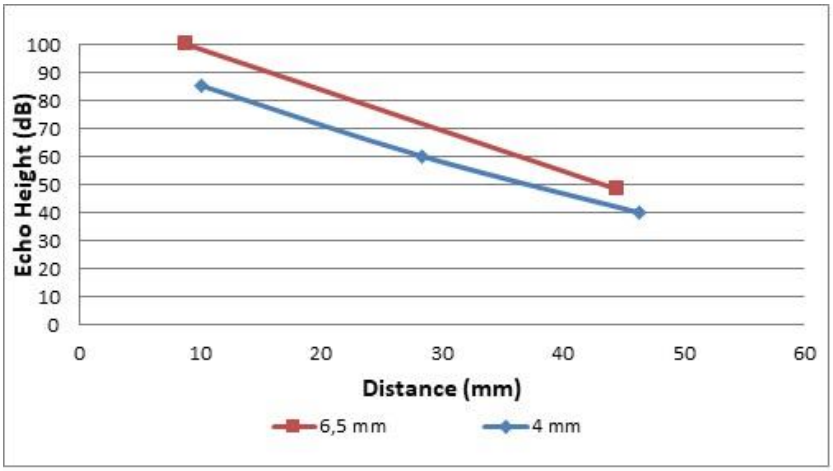

Figure 15. Experimental findings for the second test specimen, illustrating the relationship between signal amplitude, hole diameter, and propagation depth.

3.3. Comparative Analysis of Flaw Detection via Normal and Angle-Beam Probes at 45°, 60°, and 70° Refraction

The comparative performance of immersion-based angle generation versus conventional contact angle-beam probes was systematically evaluated for the third specimen. The resulting data, characterizing the relationship between signal amplitude and propagation distance, are quantitatively presented in Figure 16, Figure 17, and Figure 18. These findings illustrate the efficacy of utilizing a normal probe in an immersion configuration to emulate the behavior of traditional angle-beam transducers. Specifically, Figure 16 benchmarks the signal response values obtained at a 45° refractive angle, juxtaposing the immersion-based results with those of the conventional contact method to assess detection sensitivity and signal-to-noise ratio (SNR) consistency.

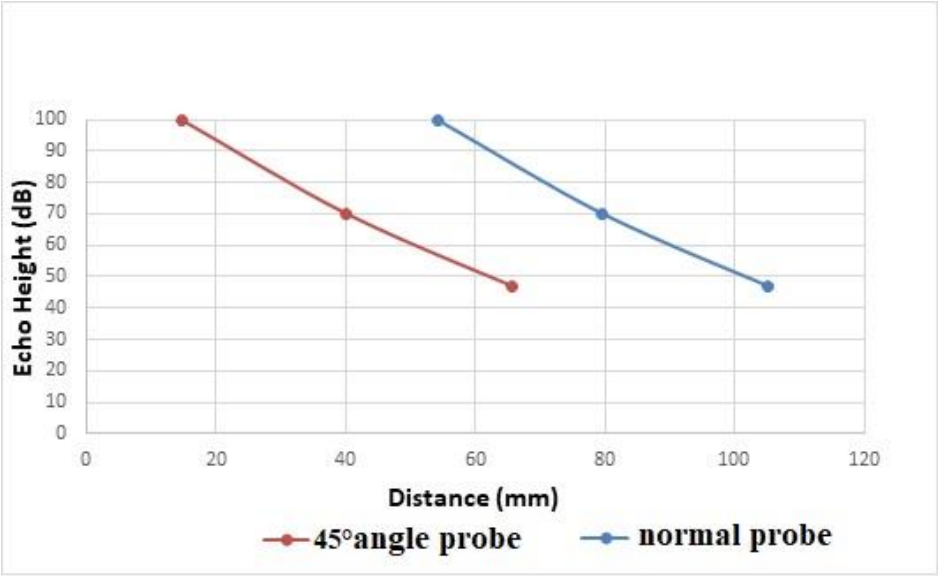

Figure 16. Comparative analysis of signal amplitude versus distance for the third test specimen at a 45° refractive angle, utilizing both immersion-based normal probe and conventional contact angle-beam probe configurations.

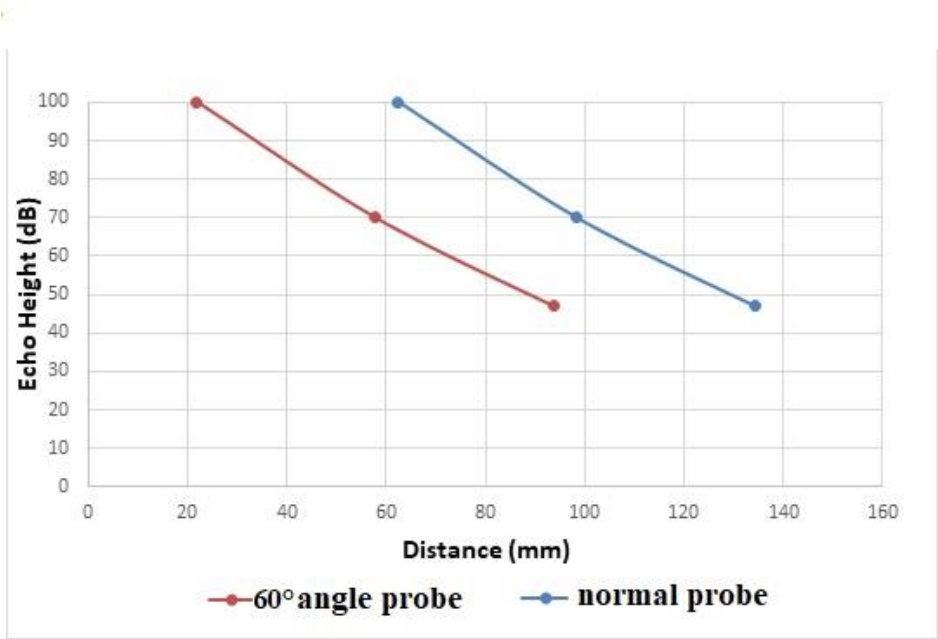

Figure 17. Comparative analysis of signal amplitude versus distance for the third test specimen at a 60° refractive angle, utilizing both immersion-based normal probe and conventional contact angle-beam probe configurations.

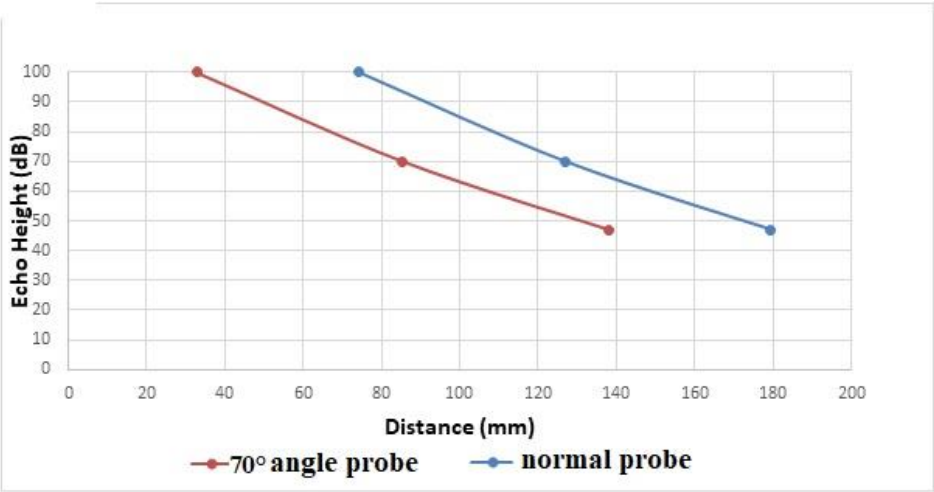

Figure 18. Comparative analysis of signal amplitude versus distance for the third test specimen at a 70° refractive angle, utilizing both immersion-based normal probe and conventional contact angle-beam probe configurations.

3.4. Comparative Discussion of Immersion and Contact Methodologies

The ultrasonic interrogation of the third specimen was executed through two distinct experimental modalities. In the first configuration, a normal (straight-beam) transducer was integrated into an immersion testing apparatus, maintaining a constant standoff distance (water path) of 17 mm between the probe face and the specimen surface. Following system calibration, the incident angle of the probe was precisely adjusted to induce refracted waves within the steel volume at target angles of 45°, 60°, and 70°. Conversely, the second modality utilized traditional 45°, 60°, and 70° angle-beam transducers. In this contact testing approach, the probes were coupled directly to the specimen surface, thereby eliminating any standoff distance.

When the immersion-based normal probe was configured for 45°, 60°, and 70° inspection, significant variations in signal arrival times and trajectories were observed compared to contact testing. These discrepancies are primarily attributed to two physical phenomena: first, the refraction of the acoustic beam as it traverses the water-steel interface, and second, the inherent mode conversion occurring at the boundary. To mitigate mode interference and ensure that the acoustic energy propagated exclusively at the intended refracted angles within the material, the transducer was oriented at incident angles of 19°, 23°, and 25°, respectively, in accordance with Snell's Law.

The experimental data indicated that the flaw distances recorded during immersion testing were consistently higher than those obtained via contact probes. This phenomenon is fundamentally linked to the acoustic velocity mismatch between the two media. While the shear wave velocity in steel is approximately 3255 m/s, the longitudinal velocity in the aqueous medium is significantly lower at 1480 m/s. Consequently, the increased travel time within the water path results in an apparent spatial extension of the flaw location on the time base. These findings underscore the critical necessity of accounting for both the velocity differential and the refraction index when utilizing normal probes for immersion-based angle-beam emulation.

A systematic analysis of the graphical data in Figure 16, Figure 17, and Figure 18 reveals that immersion-based scans required a substantial increase in gain (decibels) to achieve signal amplitudes equivalent to those of contact testing. This requirement is primarily due to the attenuation and beam divergence occurring across the 17 mm standoff distance. Furthermore, a spatial deviation of approximately 40 mm in flaw localization was observed in immersion scans relative to contact-beam measurements. This deviation is a direct consequence of the lower acoustic velocity in water, combined with the physical standoff distance between the transducer and the specimen.

These results highlight that precise temporal and spatial compensation is mandatory in immersion UT protocols to ensure diagnostic accuracy and reliable flaw characterization.

3.5. Echo Amplitude Analysis of the Fourth Specimen Set via Contact Testing

The echo amplitude characteristics for the fourth set of specimens, obtained through contact testing with a normal (straight-beam) probe, are quantitatively detailed in Figure 19. To establish a normalized reference, the first backwall echo of the 30 mm specimen was adjusted to 100% Full Screen Height (FSH) by setting the device gain to 51 dB. At a total propagation distance of 90 mm (corresponding to the third backwall reflection), the signal amplitude was observed to attenuate to 20%.

For the 49 mm specimen, a gain of 59 dB was required to achieve the 100% FSH reference level, with the signal amplitude subsequently dropping to 20% at a propagation distance of 147 mm. In the case of the 71 mm specimen, the gain was further increased to 69 dB to maintain the 100% FSH baseline; at a distance of 223 mm, the echo height similarly declined to 20%. These experimental results demonstrate a clear inverse correlation between specimen thickness and signal amplitude. As material thickness increases, the acoustic energy undergoes greater attenuation, necessitating a systematic increase in gain (dB) to compensate for the loss in signal intensity and maintain diagnostic sensitivity.

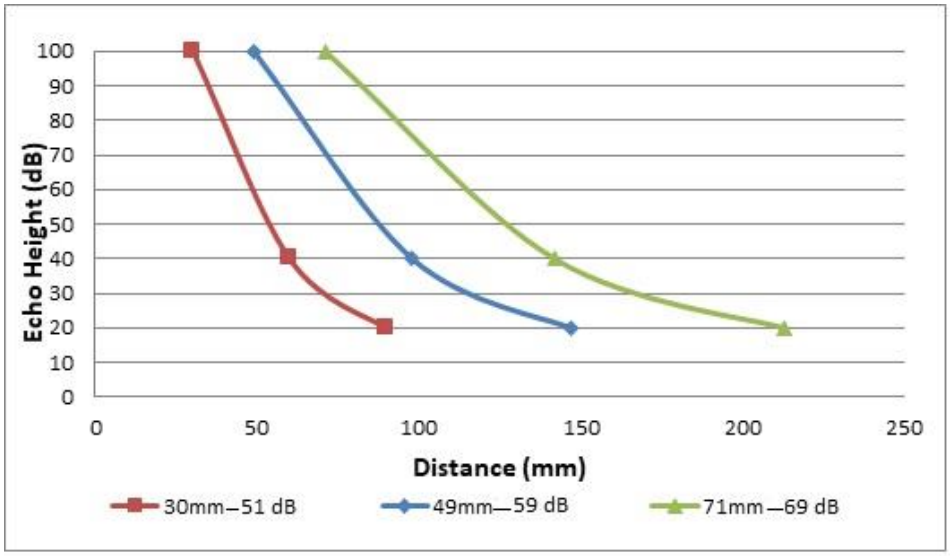

Figure 19. Experimental results and echo amplitude characteristics obtained from the contact-based ultrasonic inspection of the fourth specimen set.

3.6. Echo Amplitude Analysis of the Fourth Specimen Set via Immersion Testing

During the immersion-based inspection of the 30 mm specimen, the instrumentation gain was adjusted to 56 dB to normalize the primary backwall echo to a 100% Full Screen Height (FSH) reference. The signal amplitude was observed to attenuate to 20% at a recorded distance of 144 mm. For the 49 mm specimen, a gain of 64 dB was necessitated to achieve the 100% FSH baseline, with the signal height dropping to 20% at a distance of 201 mm. Similarly, for the 71 mm specimen, the gain was increased to 74 dB to maintain the 100% reference level, resulting in a 20% amplitude at 267 mm. A consistent characteristic was identified across the three specimens of varying heights: the second backwall echoes were consistently recorded at 40% FSH, while the third backwall reflections attenuated to 20% FSH. The significant elongation of these echo distances on the time base is fundamentally attributed to the fact that the acoustic velocity in water is approximately one-fourth of the longitudinal velocity in steel.

The synthesis of results from both experimental sets confirms that, for a constant gain level, signal amplitude is inversely proportional to material thickness. Furthermore, the study established that immersion-based inspections require a systemic gain increment of 5 dB relative to the parameters recorded during contact testing for specimens of equivalent height to achieve comparable signal response. The experimental findings and echo amplitude characteristics obtained from the immersion-based ultrasonic inspection of the fourth specimen set are graphically illustrated in Figure 20.

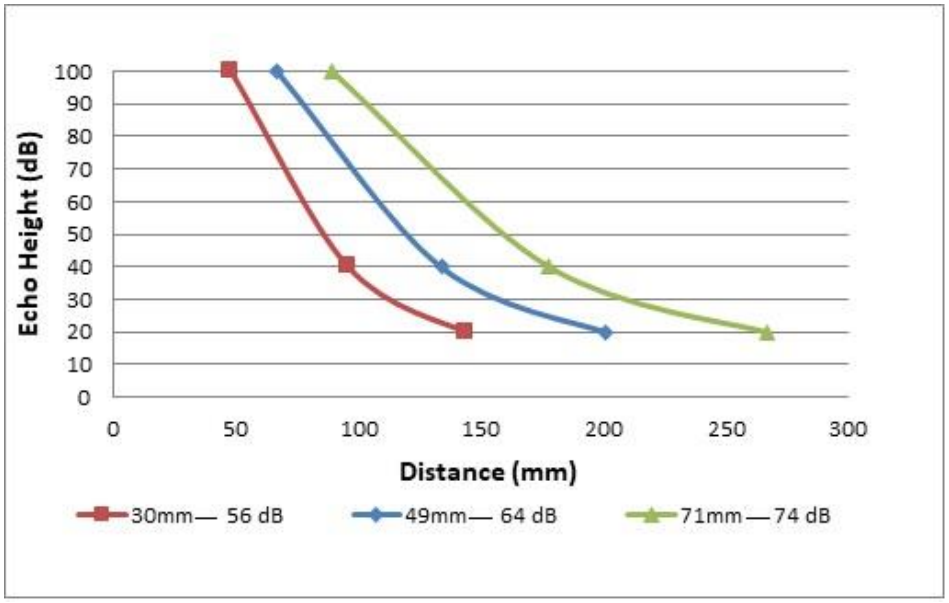

Figure 20. Experimental results and echo amplitude characteristics obtained from the contact-based ultrasonic inspection of the fourth specimen set.

4. Conclusion

In the scope of this research, the ultrasonic inspection performances of normal and angle-beam transducers were comparatively analyzed under both contact and immersion testing conditions. The experimental findings demonstrate that, provided appropriate testing geometry and acoustic calibration parameters are established, normal transducers possess the capacity to generate refracted angled waves and can serve as an effective alternative to traditional angle-beam probes for specific industrial applications.

In contact ultrasonic testing, while the utilization of normal probes offers operational flexibility and equipment accessibility, signal amplitudes exhibited fluctuations contingent upon surface conditions and couplant interaction. Conversely, traditional angle-beam probes demonstrated a more stable signal response against variations in contact conditions, thereby confirming their superior reliability for field applications. These results underscore that for critical in-situ inspections, conventional angle-beam transducers remain the primary choice.

Experimental observations revealed that angular scanning with normal probes leads to signal complexity (interference) due to the simultaneous coexistence of longitudinal and shear wave modes. To minimize methodological interference and ensure that the material is examined solely using shear waves—consistent with the use of angle-beam probes—we determined that the incident angle of the normal probe should be optimized within the range of 15° to 27°.

Taking a comprehensive approach, modifying standard probes for use in angle-beam configurations offers significant strategic benefits. This adaptation not only enhances cost-effectiveness by minimizing the need for specialized equipment but also reduces the diversity of tools required for various applications. Furthermore, it fosters greater experimental flexibility, allowing researchers to efficiently tailor their methodologies to suit a wide range of scenarios and objectives. Ultimately, it is clear that traditional angle-beam probes hold a distinct technical

advantage for inspecting structural components with intricate geometries and critical weldments, where high sensitivity is paramount.

This research introduces a complementary and alternative methodological approach to the non-destructive testing (NDT) literature. In future projections, additional experiments involving broader frequency spectra, diverse material types, and autonomous robotic scanning systems are expected to contribute to a more comprehensive evaluation of the method's industrial applicability and reliability.

Finally, analysis conducted via the immersion method established that, due to the lower propagation velocity and attenuation characteristics of acoustic waves within the liquid medium, a systematic increment in instrument gain (dB) and precise temporal compensation are mandatory compared to contact testing parameters to ensure diagnostic accuracy.

Author contributions

Cenap Güven: Conceptualization, Methodology, Data curation, Software, Writing-Reviewing and Editing.
Cengiz Doğan: Data curation, Management, Writing-Reviewing and Editing.

Conflicts of interest

The author declares no conflicts of interest.

References

1. Krautkrämer, J., & Krautkrämer, H. (2013). *Ultrasonic testing of materials*. Springer-Verlag.
2. Blitz, J., & Simpson, G. (1996). *Ultrasonic methods of non-destructive testing*. Chapman & Hall.
3. Hellier, C. (2013). *Handbook of nondestructive evaluation* (2nd ed.). McGraw-Hill Education.
4. Bond, L. J. (2018). *Fundamentals of ultrasonic inspection*. (Technical Handbook Series).
5. Rifai, D., Abdalla, A. N., Ali, K., & Razali, R. (2016). Giant magnetoresistance sensors: A review on structures and non-destructive eddy current testing applications. *Sensors, 16*(3), 298.
6. Gholizadeh, S. (2016). A review of non-destructive testing methods of composite materials. *Procedia Structural Integrity, 1*, 50–57.
7. ASM International. (2018). *Nondestructive evaluation and quality control*. ASM Handbook (Vol. 17). ASM International.
8. ASTM International. (2015). *Standard practice for ultrasonic pulse-echo straight-beam examination by the contact method* (ASTM E114-15).
9. Scott, I. G., & Scala, C. M. (1982). A review of non-destructive testing of composite materials. *NDT International, 15*(2), 75–86.
10. Obadimu, S. O., McLaughlin, J., & Kourousis, K. I. (2023). Immersion ultrasonic testing of artificially induced defects in fused filament fabricated steel 316L. *3D Printing and Additive Manufacturing, 10*(1), 34–39.
11. Durmaz, T., Bandaru, A. K., & O'Higgins, R. M. (2025). Non-destructive evaluation of induced defects in aerospace-grade CFRP composites using immersion ultrasonic C-scan. *Results in Engineering, 25*, 108333.
12. EN ISO 16810. (2012). *Non-destructive testing — Ultrasonic testing — General principles*.
13. EN ISO 17640. (2018). *Non-destructive testing of welds — Ultrasonic testing — Techniques, testing levels, and assessment*.
14. ASTM International. (2013). *Standard practice for contact ultrasonic testing of weldments* (ASTM E164-13).
15. Schmerr, L. W. (2016). *Fundamentals of ultrasonic nondestructive evaluation: A modeling approach*. Springer.
16. Drinkwater, B. W., & Wilcox, P. D. (2006). Ultrasonic arrays for non-destructive evaluation: A review. *NDT & E International, 39*(7), 525–541.
17. Güven, C. (2014). *Su altı ultrasonik test düzeneği tasarımı ve imalatı / Underwater ultrasonic test apparatus design and manufacturing* (Doctoral dissertation)